NANO LETTERS

pubs.acs.org/NanoLett

DNA Translocation through Graphene Nanopores

Grégory F. Schneider, Stefan W. Kowalczyk, Victor E. Calado, Grégory Pandraud, Henny W. Zandbergen, Lieven M. K. Vandersypen, and Cees Dekker*

Kavli Institute of Nanoscience, Lorentzweg 1, 2628 CJ Delft, The Netherlands

ABSTRACT Nanopores—nanosized holes that can transport ions and molecules—are very promising devices for genomic screening, in particular DNA sequencing. Solid-state nanopores currently suffer from the drawback, however, that the channel constituting the pore is long, ~100 times the distance between two bases in a DNA molecule (0.5 nm for single-stranded DNA). This paper provides proof of concept that it is possible to realize and use ultrathin nanopores fabricated in graphene monolayers for single-molecule DNA translocation. The pores are obtained by placing a graphene flake over a microsize hole in a silicon nitride membrane and drilling a nanosize hole in the graphene using an electron beam. As individual DNA molecules translocate through the pore, characteristic temporary conductance changes are observed in the ionic current through the nanopore, setting the stage for future single-molecule genomic screening devices.

KEYWORDS Graphene, nanopore, wedging transfer, translocation, DNA, sequencing

In the past few years, nanopores have emerged as a new powerful tool to interrogate single molecules.[1−3] They have been successfully used to rapidly characterize biopolymers like DNA,[4,5] RNA,[6] as well as DNA−ligand complexes[7] and local protein structures along DNA[8] at the single-molecule level. A key driving force for nanopore research in the past decade has been the prospect of DNA sequencing. However, a major roadblock for approaching high-resolution DNA sequencing with pores is the finite length of the channel constituting the pore (Figure 1A). In a typical solid-state nanopore in say a 30 nm thick membrane, the current blockade resulting from DNA translocation is due to a large number of bases (~100) present in the pore. Here, we demonstrate that this limitation can be overcome by realizing an ultimately thin nanopore device, that is, two aqueous flow chambers separated by a nanopore in a graphene monolayer. Furthermore, we show the translocation of individual DNA molecules through such graphene nanopores. Fabrication of nanopores in graphene layers was reported previously in the vacuum of a transition electron microscope (TEM),[9,10] but graphene nanopore devices that ionically probe the translocation of single molecules were so far not realized.

Graphene is a two-dimensional layer of carbon atoms packed into a honeycomb lattice with a thickness of only one atomic layer (~0.3 nm).[11] Despite its minimal thickness, graphene is robust as a free-standing membrane.[12,13] In addition, graphene is a very good electrical conductor.[14] Graphene therefore opens up new opportunities for nanopores such as new analytical platforms to detect, for example, local protein structures on biopolymers or sequencing with single-base resolution. Indeed, theoretical calculations of DNA translocation through a nanopore in graphene have already indicated the possibility for single-base resolution by probing the translocating molecule electrically in the transverse direction by use of the intrinsic conductive properties of graphene.[15]

We obtain single-layer graphene (Figure 1B) by mechanical exfoliation from graphite on SiO_2.[16] We preferred graphene obtained by mechanical exfoliation over synthetic graphene[17] because it contains fewer defects and it allows to select graphene sheets with a range of thicknesses (i.e.,

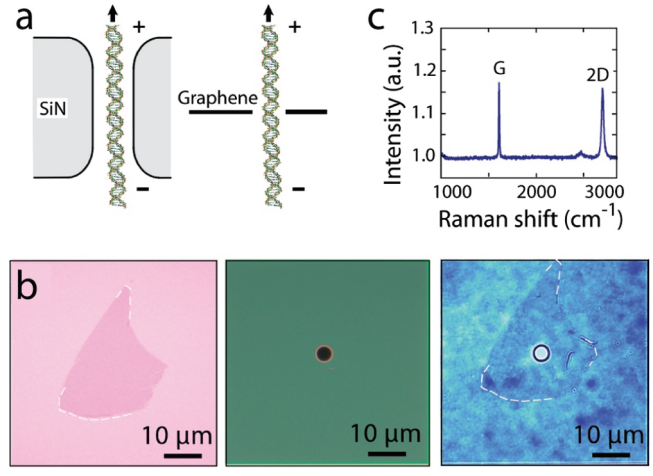

FIGURE 1. Graphene nanopores for DNA translocation (A) To-scale side-view illustration comparing DNA translocation through a SiN solid-state nanopore with that through a free-standing one-atom-thick graphene nanopore. (B) Optical micrographs depicting the transfer of graphene from Si/SiO_2 (left) onto a microfabricated silicon nitride chip containing a 5 μm hole (right). After the transfer by wedging, the flake entirely covers the hole. (C) Raman spectrum of the flake on Si/SiO_2 before the transfer.

* Corresponding author, c.dekker@tudelft.nl.
Received for review: 06/11/2010
Published on Web: 07/07/2010

DOI: 10.1021/nl102069z | *Nano Lett.* **2010,** *10,* 3163–3167

number of layers). Monolayer graphene is identified by its particular optical contrast[18] in the optical microscope and by Raman measurements (Figure 1C). At ~1590 cm^{-1}, we measure the so-called G resonance peak and at ~2690 cm^{-1} the 2D resonance peak. In the case of multilayer graphene, the 2D resonance peak splits off in multiple peaks in contrast to monolayer graphene which has a very sharp single resonance peak. In this way, we are well able to distinguish single-layer graphene from multilayer graphene.[19]

We select a monolayer of graphene and transfer it onto a SiN support membrane with a 5 μm sized hole[20] by use of our recently developed "wedging transfer" technique.[21] This transfer procedure is straightforward: flakes can be overlaid to support membranes in less than an hour. Briefly, a hydrophobic polymer is spun onto a hydrophilic substrate (here plasma-oxidized SiO_2) with graphene flakes, and wedged off the substrate by sliding it at an angle in water. Graphene flakes are peeled off the SiO_2 along with the polymer. The polymer is then floating on the water surface, located near a target SiN substrate, the water level is lowered, and the flakes are positioned onto the SiN membrane with micrometer lateral precision. In the final step the polymer is dissolved.

We then drill a nanopore into the graphene monolayer using the highly focused electron beam of a transmission electron microscope (TEM). The acceleration voltage is 300 kV, well above the 80−140 kV knockout voltage for carbon atoms in graphene[22] (see Methods). Drilling the holes by TEM is a robust well-reproducible procedure (we drilled 39 holes with diameters ranging from 2 to 40 nm, in monolayer as well as in multilayer graphene; some examples of pores are shown in Figure 2). Because of the high acceleration voltage of the electron beam, drilling could potentially induce damage to the graphene around the pore. However, electron beam diffraction measurements across the hole (Figure 2B,C) confirm the crystallinity of the monolayer surrounding the hole, as evidenced by the well-defined hexagonal diffraction patterns (Figure 2C).

Subsequently, we mount the pore into a microfluidic flow cell, add a 1 M saline solution (1 M KCl, room temperature (TE), pH 8.0) on both sides of the graphene membrane, and measure current−voltage ($I-V$) curves from ion transport through the graphene nanopore (inset of Figure 3). The resistance value (5.1 MΩ in the example of the inset of Figure 3) and the linearity of the $I-V$ curve indicate that the current is consistent with ion flow through the pore and does not arise from electrochemical processes at the conductive graphene surface.[23] Furthermore, samples with a graphene layer but without a nanopore exhibit a very high ionic resistance (>10 GΩ), which indicates that the graphene flake adheres well to the SiN surface and forms an insulating seal.

We measured $I-V$ curves for a number of pores ranging from 5 to 25 nm in diameter, in six monolayer graphene devices and seven multilayer graphene devices. Sample thickness is determined based on transmitted light intensity

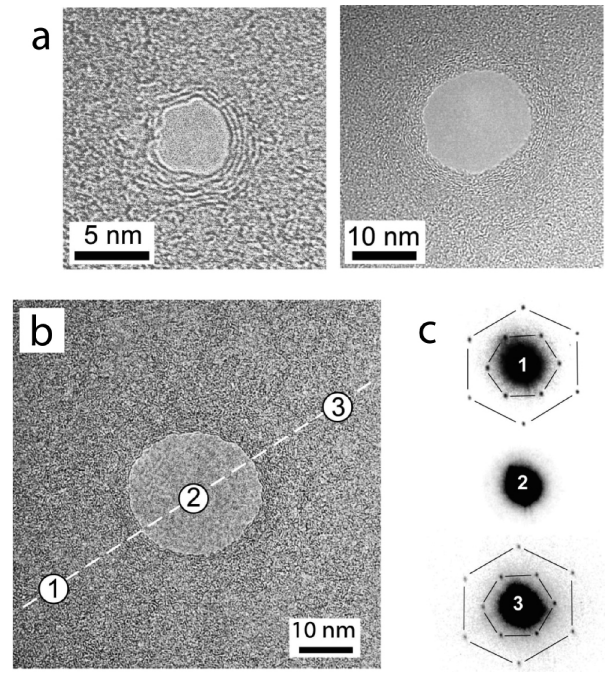

FIGURE 2. Drilling of graphene nanopores. (A) Transmission electron microscopy (TEM) of some nanopores drilled into multilayer graphene (B) TEM image of a 22 nm diameter pore in monolayer graphene. Incrusted numbers indicate spots where the diffraction patterns were recorded. (C) Diffraction patterns measured across the monolayer nanopore of panel B. The diffraction pattern was measured at three spots—indicated in panel B—with a 3 nm electron beam. The hexagonal lattice of diffraction spots is highlighted by the solid lines for clarity.

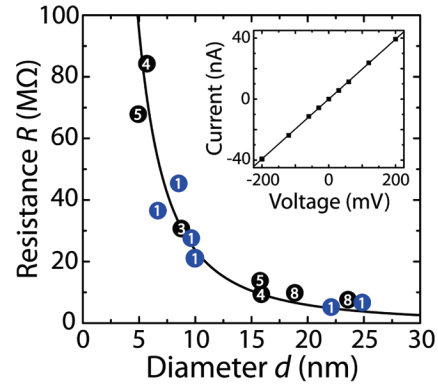

FIGURE 3. Nanopore resistances. Measured values of pore resistance versus diameter for 13 graphene nanopores. For each pore, the number of graphene layers is indicated by the number within the circle: "1" denotes graphene monolayers (blue); "*x*" denotes *x* layers of graphene (black). The solid line denotes a $1/d^2$ dependence. The inset shows an $I-V$ curve of a 22 nm nanopore in a graphene monolayer recorded in 1 M KCl. A linear resistance of 5.1 MΩ is observed.

(2.3% reduction per layer).[24] Figure 3 shows the obtained resistances versus pore diameter, for both monolayers and multilayers up to eight layers (with a total layer thickness between 0.3 and 2.7 nm). We do not observe a strong dependence on the number of layers constituting the nanopore membrane. Note that these data are all taken in the

DOI: 10.1021/nl102069z | *Nano Lett.* **2010,** *10,* 3163–3167

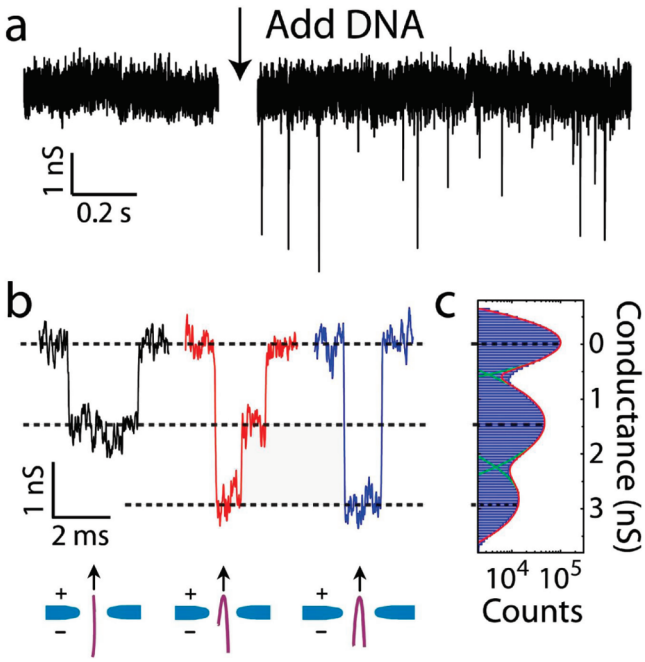

FIGURE 4. DNA translocation through a nanopore in a graphene monolayer. (A) Translocation of 48 kbp double-stranded λ-DNA across a 22 nm nanopore within a graphene monolayer, showing the baseline conductance (left) and blockade events upon addition of DNA (right). (B) Examples of translocation events of nonfolded (black), partially folded (red), and fully folded (blue) DNA molecules recorded at 200 mV in the 22 nm pore represented in Figure 3. (C) Conductance histogram collected from 1222 translocation events, including the open-pore conductance before and after the event.

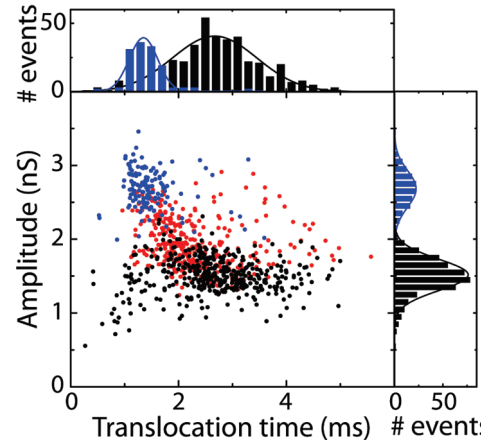

FIGURE 5. Scatter diagram of the amplitude of the conductance blockade versus translocation time for DNA translocation through a 22 nm diameter nanopore in a graphene monolayer. The accompanying histograms for the nonfolded and fully folded data are included at the top and the right. Color coding is as Figure 4. Each point in this scatter diagram corresponds to a single translocation event. Applied voltage is 200 mV.

regime where the pore diameter is much larger than the thickness of the graphene membrane. We determined how the pore resistance R scales with the pore diameter d, by fitting the diameter dependence of the resistance and conductance with a variety of functional dependences (see Supporting Information for an extensive discussion of these fits). Surprisingly, we find that the dependence of pore resistance R on diameter d is better described by $R \sim 1/d^2$, which is the expected behavior for a cylindrical pore, than by a $R \sim 1/d$ dependence, which would be expected if the access resistance dominates.[25] Since the membrane thickness is smaller than the pore diameter, we would have expected the access resistance of the pore to dominate the total resistance. A crossover between a $1/d$ and $1/d^2$ dependence or other functional dependencies cannot be excluded with the current data (see Supporting Information).

Double-stranded DNA (dsDNA) can be driven electrophoretically through the nanopore and detected by monitoring the ion current. Upon addition of the λ-dsDNA (16 μm long) on one side of the pore and applying a voltage of 200 mV across the graphene membrane, a series of spikes is observed in the conductance traces (Figure 4A). Each temporary drop in the measured conductance, ΔG, arises from a single DNA molecule that translocates through the pore. As for conventional SiN nanopores,[26] three characteristic signals are observed, corresponding to three types of translocation events: nonfolded (where the molecule translocates in a linear head-to-tail fashion), partially folded (where the molecule is randomly grabbed from the side of the DNA coil, and first translocates in a singly folded fashion), or fully folded molecules (where the DNA happens to be grabbed in the middle of the molecule).[5] Example events are shown in Figure 4B. The events are color coded in black (nonfolded), red (partially folded), and blue (fully folded). From a large number ($n = 1222$) of such events, we obtain a histogram of conductance blockade levels ΔG, as presented in Figure 4C. Three peaks are visible, the first being the open-pore current at 0 nS (i.e., the baseline); the peak at $\sim$1.5 nS which corresponds to one strand of DNA in the pore; and the peak at $\sim$3 nS due to two strands of the same DNA molecule in the pore. We measured DNA translocations on seven graphene nanopores (monolayer and multilayer graphene membranes with pore diameters ranging from 10 to 25 nm) and collected good statistics on three devices (two monolayers and an eight-layer multilayer with pore diameters of 22, 25, and 24 nm, respectively).

A scatter plot of ΔG versus the time duration of the events is shown in Figure 5, with the same color coding as used in Figure 4B. Each dot in this diagram represents a single DNA translocation event. The blockade amplitude $\Delta G = 1.5 \pm 0.4$ nS for nonfolded DNA in these graphene pores is quite similar in magnitude to that measured for pores of similar sizes in a 20 nm thick SiN membrane (1.4 ± 0.3 nS) for the same conditions.[27] This is unexpected as we would expect the ionic current blocked by a DNA molecule to scale as the inverse of the thickness of the nanopore membrane,[22] leading to higher blockade amplitudes for DNA in graphene pores.

In addition to the event amplitude, we studied the translocation times of the events. The average translocation time

DOI: 10.1021/nl102069z | Nano Lett. 2010, 10, 3163–3167

is 2.7 ± 0.8 ms for the nonfolded DNA (Figure 5), a value that is similar, albeit slightly larger, to that for solid-state nanopores in a 20 nm SiN membrane for which the translocation time is 1.2 ± 0.3 ms under the same applied voltage of 200 mV and for a similar pore diameter.[27] A slightly larger translocation time compared to SiN pores was also observed for our other monolayer device for which we also got good statistics. We note that the translocation time is expected to be independent of the membrane thickness because the driving electrostatic force is the same: in a thinner membrane, the electric field over the graphene pore is higher (same voltage applied over a shorter distance) which however is exactly compensated by the smaller number of charges present on the piece of the DNA molecule that resides in the pore.[28] This is only a crude scaling argument however, and there can be various reasons why the translocation time is somewhat different for ultrathin nanopores. At a practical level, a slower translocation will be helpful for analytical applications where maximizing spatial resolution is needed.

The establishment of double-stranded DNA translocation through single-layer graphene nanopores represents an important first step toward pushing the spatial-resolution limits of single-molecule nanopore analytics to subnanometer accuracy. Future research will be aimed at exploring single-strand DNA translocation, single-base detection, and ultimately sequencing.

Methods. ***Preparation of Graphene Samples for Wedging Transfer.*** We prepared graphene sheets on clean and freshly plasma-oxidized (O_2, Diener) Si/SiO_2 substrates by mechanical exfoliation of natural graphite (NGS Naturgraphit GmbH) with blue NITTO tape (SPV 224P). The plasma serves to make the substrate hydrophilic, which is needed for the wedging transfer. To render graphene monolayers visible, we used Si/SiO_2 wafers with a 90 nm thermally grown SiO_2 layer (IDB Technologies). We located the single and few layer graphene sheets under an optical microscope and identified the number of layers by their optical contrast as well as by Raman spectroscopy. Graphene flakes were transferred onto microfabricated Si/SiO_2/SiN chips described before.[20] We used cellulose acetate butyrate (Sigma-Aldrich) dissolved in ethyl acetate (30 mg/mL) as the transfer polymer.[18] Contrary to the design described by Krapf et al., prior the transfer of graphene, we etched the 20 nm thin SiN membrane using hot phosphoric acid (200 °C) for 45 min.

Transmission Electron Microscopy and Fabrication of Nanopores in Graphene. Nanopores were fabricated and imaged using a Cs-corrected Titan Cubed Supertwin/STEM FP5600/40 microscope operated at an accelerating voltage of 300 kV. An electron beam with a diameter of 15 nm at full width at half-maximum height and a beam density of 10^6 electrons/(s · nm^2) was used for drilling. Gatan 2k × 2k CCD with binning 1 was used for image recording. Diffraction patterns were acquired with a beam size of 3 nm and a beam density of 10^5 electrons/(s · nm^2). To remove contamination, samples were heated at 200 °C for at least 20 min prior to their insertion in the vacuum chamber of the microscope. After being drilled, samples were stored in ethanol.

Nanopore Experiments. For the electrical measurements, a membrane with a single graphene nanopore is mounted in a polyether ether ketone (PEEK) microfluidic flow cell and sealed to liquid compartments on either side of the sample. Measurements are performed in 1 M KCl salt solution containing 10 mM Tris−HCl and 1 mM EDTA at pH 8.0 at room temperature (or TE, as abbreviated in the manuscript). Ag/AgCl electrodes are used to detect ionic currents and to apply electric fields. Current traces are measured at 100 kHz bandwidth using a resistive feedback amplifier (Axopatch 200B, Axon Instruments) and digitized at 500 kHz. Before dsDNA was injected, the graphene-SiN-microchip was flushed with a 1 mg/mL solution of 16-mercaptohexadecanoic acid in 8:2 toluene/ethanol and additionally rinsed in respectively clean 8:2 toluene/ethanol and ethanol. This is expected to form a flat self-assembled monolayer on the graphene surface which demotes DNA adhesion (this treatment is not mandatory to observe DNA translocations).[29] dsDNA was unmethylated λ-DNA (20 ng/μL, reference no. D152A, lot no. 27420803, Promega, Madison, WI). The event-fitting algorithm used to analyze and label the translocation events was the same as the one described before.[5] Only events exceeding six times the standard deviation of the open-pore root-mean-square noise are considered. Due to possible baseline fluctuations, we only considered events whose current before and after the event does not change more than 10% of the event amplitude. We additionally filtered the data at 10 kHz for better signal-to-noise ratio, and we discarded events shorter than 200 μs.

Acknowledgment. We thank M.-Y. Wu and Q. Xu for their assistance in TEM, H. Postma for discussions, V. Karas and K. van Schie for technical assistance, and The Netherlands Organisation for Scientific Research (NWO), the NanoSci-E+ Program, the Foundation for Fundamental Research on Matter (FOM), and the EC project READNA for funding.

Supporting Information Available. Ionic resistance and conductance for graphene nanopores of various diameters, fitted according to different functional dependences, and table of fit functions and corresponding fit parameters. This material is available free of charge via the Internet at http://pubs.acs.org.

REFERENCES AND NOTES

(1) Branton, D.; Deamer, D. W.; Marziali, A.; Bayley, H.; Benner, S. A.; Butler, T.; Di Ventra, M.; Garaj, S.; Hibbs, A.; Huang, X. H.; Jovanovich, S. B.; Krstic, P. S.; Lindsay, S.; Ling, X. S. S.; Mastrangelo, C. H.; Meller, A.; Oliver, J. S.; Pershin, Y. V.; Ramsey, J. M.; Riehn, R.; Soni, G. V.; Tabard-Cossa, V.; Wanunu, M.; Wiggin, M.; Schloss, J. A. *Nat. Biotechnol.* **2008**, *26*, 1146–1153.
(2) Dekker, C. *Nat. Nanotechnol.* **2007**, *2*, 209–215.
(3) Ma, L.; Cockroft, S. L. *ChemBioChem* **2010**, *11*, 25–34.

DOI: 10.1021/nl102069z | *Nano Lett.* **2010,** *10,* 3163–3167

(4) Li, J. L.; Gershow, M.; Stein, D.; Brandin, E.; Golovchenko, J. A. *Nat. Mater.* **2003**, *2*, 611–615.
(5) Storm, A. J.; Storm, C.; Chen, J. H.; Zandbergen, H.; Joanny, J. F.; Dekker, C. *Nano Lett.* **2005**, *5*, 1193–1197.
(6) Skinner, G. M.; van den Hout, M.; Broekmans, O.; Dekker, C.; Dekker, N. H. *Nano Lett.* **2009**, *9*, 2953–2960.
(7) Wanunu, M.; Sutin, J.; Meller, A. *Nano Lett.* **2009**, *9*, 3498–3502.
(8) Kowalczyk, S. W.; Hall, A. R.; Dekker, C. *Nano Lett.* **2010**, *10*, 324–328.
(9) Fischbein, M. D.; Drndic, M. *Appl. Phys. Lett.* **2008**, *93*, 113107.
(10) Girit, C. O.; Meyer, J. C.; Erni, R.; Rossell, M. D.; Kisielowski, C.; Yang, L.; Park, C. H.; Crommie, M. F.; Cohen, M. L.; Louie, S. G.; Zettl, A. *Science* **2009**, *323*, 1705–1708.
(11) Novoselov, K. S.; Geim, A. K.; Morozov, S. V.; Jiang, D.; Zhang, Y.; Dubonos, S. V.; Grigorieva, I. V.; Firsov, A. A. *Science* **2004**, *306*, 666–669.
(12) Tsoukleri, G.; Parthenios, J.; Papagelis, K.; Jalil, R.; Ferrari, A. C.; Geim, A. K.; Novoselov, K. S.; Galiotis, C. *Small* **2009**, *5*, 2397–2402.
(13) Meyer, J. C.; Geim, A. K.; Katsnelson, M. I.; Novoselov, K. S.; Booth, T. J.; Roth, S. *Nature* **2007**, *446*, 60–63.
(14) Castro Neto, A. H.; Guinea, F.; Peres, N. M. R.; Novoselov, K. S.; Geim, A. K. *Rev. Mod. Phys.* **2009**, *81*, 109–162.
(15) Postma, H. W. C. *Nano Lett.* **2010**, *10*, 420–425.
(16) Novoselov, K. S.; Jiang, D.; Schedin, F.; Booth, T. J.; Khotkevich, V. V.; Morozov, S. V.; Geim, A. K. *Proc. Natl. Acad. Sci. U.S.A.* **2005**, *102*, 10451–10453.
(17) Park, S.; Ruoff, R. S. *Nat. Nanotechnol.* **2009**, *4*, 217–224.
(18) Blake, P.; Hill, E. W.; Neto, A. H. C.; Novoselov, K. S.; Jiang, D.; Yang, R.; Booth, T. J.; Geim, A. K. *Appl. Phys. Lett.* **2007**, *91*, No. 063124.
(19) Ferrari, A. C.; Meyer, J. C.; Scardaci, V.; Casiraghi, C.; Lazzeri, M.; Mauri, F.; Piscanec, S.; Jiang, D.; Novoselov, K. S.; Roth, S.; Geim, A. K. *Phys. Rev. Lett.* **2006**, *97*, 187401.
(20) Krapf, D.; Wu, M. Y.; Smeets, R. M. M.; Zandbergen, H. W.; Dekker, C.; Lemay, S. G. *Nano Lett.* **2006**, *6*, 105–109.
(21) Schneider, G. F.; Calado, V. E.; Zandbergen, H. W.; Vandersypen, L. M. K., C. D. *Nano Lett.* **2010**, *10*, 1912–1916.
(22) Hashimoto, A.; Suenaga, K.; Gloter, A.; Urita, K.; Iijima, S. *Nature* **2004**, *430*, 870–873.
(23) Heller, I.; Chatoor, S.; Mannik, J.; Zevenbergen, M. A. G.; Oostinga, J. B.; Morpurgo, A. F.; Dekker, C.; Lemay, S. G. *Nano Lett.* **2010**, *10*, 1563–1567.
(24) Nair, R. R.; Blake, P.; Grigorenko, A. N.; Novoselov, K. S.; Booth, T. J.; Stauber, T.; Peres, N. M. R.; Geim, A. K. *Science* **2008**, *320*, 1308–1308.
(25) Hall, J. E. *J. Gen. Physiol.* **1975**, *66*, 531–532.
(26) Wu, M. Y.; Smeets, R. M. M.; Zandbergen, M.; Ziese, U.; Krapf, D.; Batson, P. E.; Dekker, N. H.; Dekker, C.; Zandbergen, H. W. *Nano Lett.* **2009**, *9*, 479–484.
(27) Kowalczyk, S. W.; et al. Unpublished.
(28) Keyser, U. F.; Koeleman, B. N.; Van Dorp, S.; Krapf, D.; Smeets, R. M. M.; Lemay, S. G.; Dekker, N. H.; Dekker, C. *Nat. Phys.* **2006**, *2*, 473–477.
(29) Xu, S. L.; Yin, S. X.; Liang, H. P.; Wang, C.; Wan, L. J.; Bai, C. L. *J. Phys. Chem. B* **2004**, *108*, 620–624.

DOI: 10.1021/nl102069z | *Nano Lett.* **2010,** *10,* 3163–3167